Non-Newtonian Effects on Flow-Generated Cavitation and on Cavitation in a Pressure Field[1]

ALBERT T. ELLIS AND ROBERT Y. TING

University of California, San Diego

Observations are presented which show that the stresses in a flow field of very dilute polymer are not well enough described by the Navier-Stokes equations to accurately predict cavitation. The constitutive equation for the particular polymer and concentration used is needed. The second-order fluid form in which accelerations are relatively important appears capable of explaining observed cavitation suppression by changing the pressure field due to flow.

Bubble dynamics in stationary dilute polymer solutions are also examined and found to be little different from those in water.

In earlier work (refs. 1 and 2), the authors reported the suppression of flow-generated cavitation in dilute polymers on cylinders with hemispherical noses at Reynolds numbers from 7×10^4 to 3.1×10^5. Reduction of the incipient cavitation number to 30 percent of its value for tap water was observed. Flow velocity field visualization was achieved by optical techniques using 1-microsecond light pulses scattered by polymer particles or small polystyrene latex spheres in the flow. Dark field multi-exposure photographs taken at 90 degrees to the direction of the light beam thus provided reliable data on velocity field magnitude and direction and ruled out the possibility of errors due to non-Newtonian effects on pressure taps. Figure 1 shows the results.

POSSIBLE MECHANISMS

While it is believed that incipient flow cavitation suppression by dilute polymers has been shown to be a real effect of considerable magnitude, the correct mechanism involved is still to be proven. The main purpose of

[1] This work was supported by the Office of Naval Research, Fluid Mechanics Branch, Contract N0014-67-A-0109-0007.

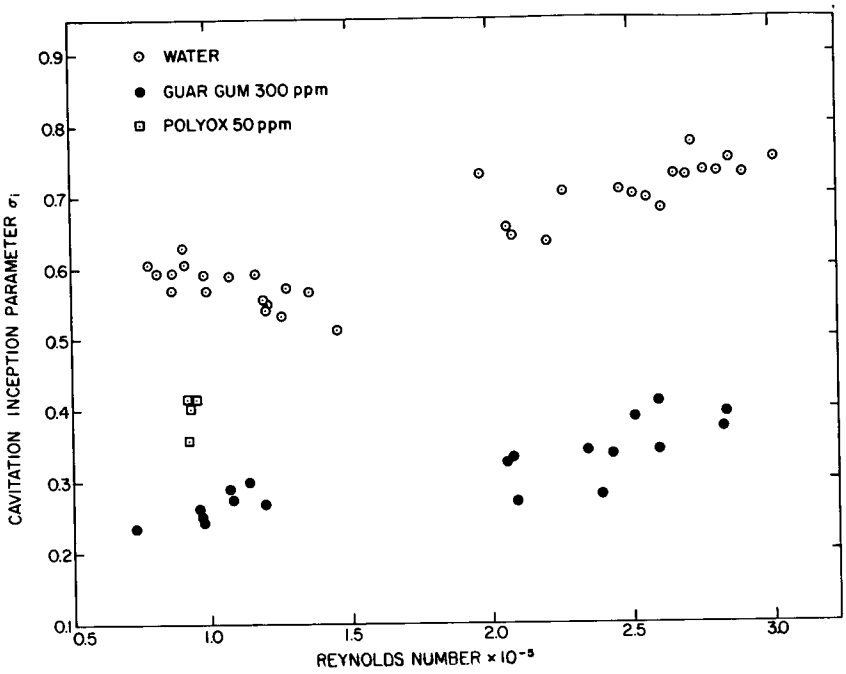

FIGURE 1.—*Cavitation inception parameter versus Reynolds number.*

this paper is to report the results of early stages of a program which, it is hoped, will accomplish this end in a systematic fashion.

It is still the opinion of the authors that cavitation suppression is due to an overpressure existing in the region of the model where the pressure would ordinarily be low enough to permit cavitation in the case of water. This belief is supported by the fact that true velocities—both around the model and along the axial streamline—obtained by the optical method are as much as 10 percent higher than the velocities calculated from the Bernoulli equation on the basis of pressure-tap readings upstream (in the upper tank of the blow-down tunnel where the liquid is quiescent) and flush with the wall of the working section. These details of the facility and instrumentation have been described elsewhere (refs. 2 and 3). The nozzle itself is based on designs of Stewart (ref. 4) and Tsien (ref. 5) to provide a nearly uniform velocity profile across the working section. Optical measurements—not including the boundary layer—indicate that the nozzle apparently does this quite well, so that the flow approaching the model is a uniform potential flow.

The absolute velocities measured by the optical technique show that the pressure at the high-velocity end of the nozzle (measured by the pressure tap flush with the wall at the working section entrance) is

approximately 10 to 18 percent higher than that for water, depending on the kind of polymers used. Over the range of 40 to 70 feet per second, the error is independent of the flow velocity. For the three different sizes of pressure taps tested—$\frac{1}{4}$, $\frac{1}{8}$, and $\frac{1}{16}$ inch in diameter—the error increases very slightly as the sizes of the pressure taps decrease. Samples from the various runs of polymers were monitored for degradation by testing drag reduction in a portable hydrating apparatus kindly supplied by Dr. Hoyt of the U.S. Naval Underseas Research Center, Pasadena. It should be especially noted that the sign of the error is positive rather than negative as has been shown to be the case for pressure-tap error both experimentally and theoretically by Professors Tanner and Pipkin (ref. 6) of Brown University for low-speed polymer flows.

It is believed by the authors that the errors observed in reference 2 are not primarily pressure-tap errors, but, rather, that the Bernoulli equation must contain a correction term. An analysis made by the authors based on the second-order fluid model for the extensional flow along the center streamline through the nozzle gives an expression for the pressure of the form:

$$P = P_N + 2\alpha \left[2 \left(\frac{du}{dx} \right)^2 - u \frac{d^2u}{dx^2} \right] \tag{1}$$

where P is the free-stream pressure and is made up of P_N, the free-stream pressure for water, and a correction term involving α, one of the material constants of the second-order fluid model represented by equation (7), (which may be different for various solutions), the velocity along the central streamline, u, and its spatial derivatives, du/dx and d^2u/dx^2. It should be noted that this correction to the pressure may thus be positive or negative. In our experiment, u, du/dx, and d^2u/dx^2 were such that, if α were given the value of -0.01 dyne sec^2/cm^2 taken as a representative value in the literature, then the pressure correction would be positive, as indicated by our working-section pressure-tap reading. It is not proposed that the second-order fluid is a correct model in all situations, but rather that the truncation in its theoretical derivation permits us to obtain a solution which may be used to explain our experimental results.

The idea that polymers may affect other than turbulent pressure fields has also been advanced by various persons such as Professor John Lumley (ref. 7) and Dr. Arndt in his discussion of the authors' previous work (ref. 2).

It was also suggested by Dr. Fabula in his discussion (ref. 2) as well as by Professor Tanner (ref. 8) that the suppression of cavitation inception might be due to effects of polymers on individual cavitation bubble growth or collapse. This possibility had also occurred to the authors, and it was therefore decided to pursue theoretical and experimental work to assess the validity of this concept. The theoretical study of a perfectly spherical

bubble is obviously attractive because of its symmetry, which greatly simplifies the analytical solution for the bubble radius as a function of time. The solution for water was obtained by Lord Rayleigh in 1917 for the case of a vapor bubble and for one containing an isothermal permanent gas (ref. 9). Many investigators have since covered more complicated aspects of the problem, such as the effect on growth of heat transfer (refs. 10, 11, and 12); the basic stability of the spherical interface (ref. 13); and the formation of jets due to pressure gradients (ref. 14), wall proximity (ref. 15), or both (ref. 16). Fortunately, for the purposes of this paper, it turns out that a spark-generated bubble in a stationary liquid at one atmosphere pressure does remain quite spherical until a rather late stage in its collapse. During this period it follows the simple Rayleigh theory very well, as demonstrated by the experimental part of this paper. Any gas from the spark simply does not have an observable effect until later stages of higher compression are reached. Of course the spark must be of short duration (one microsecond in this case) so that thermal equilibrium is attained when maximum radius is reached. Theoretical curves are not given for the growth phase, since the simple theory used may not apply to the experiments. However, any marked effect due to extensional flow or viscoelastic effects should show up during collapse as well as growth, and the authors have therefore confined their attention to this regime.

THEORETICAL STUDY OF BUBBLE COLLAPSE

Consider the problem of a single bubble collapsing in an incompressible liquid of infinite extent. The vapor bubble is taken to be spherical at all times. Gravity effect is neglected. Thermal equilibrium is assumed such that the vapor pressure inside the bubble is uniform and equal to the equilibrium vapor pressure of the liquid at the liquid temperature. Spherical coordinates are chosen with the origin at the center of the bubble, which is at rest. The radius of the bubble at any time t is $R=R(t)$, and r is the radial distance to any point in the liquid as a spherical coordinate system (r, θ, φ) is taken. The velocity will only have one component in the radial direction, i.e.,

$$\boldsymbol{V}=u\boldsymbol{e}_r \tag{2}$$

For an incompressible liquid, the continuity equation is

$$\frac{\partial u}{\partial r}+\frac{2u}{r}=0 \tag{3}$$

which gives

$$u = u(r, t) = \frac{f(t)}{r^2} \tag{4}$$

For the bubble dynamics problem it is generally given as

$$u = \frac{R^2(t)\dot{R}(t)}{r^2} \tag{5}$$

The governing equation of motion is

$$\rho \frac{\partial u}{\partial t} + \rho u \frac{\partial u}{\partial r} = -\frac{\partial p}{\partial r} + \frac{\partial \sigma_{rr}}{\partial r} + \frac{2\sigma_{rr} - \sigma_{\theta\theta} - \sigma_{\varphi\varphi}}{r} \tag{6}$$

where p is the hydrostatic pressure and σ_{rr}, $\sigma_{\theta\theta}$, and $\sigma_{\varphi\varphi}$ are the normal stress components of the deviatory stress tensor $[\sigma_{ij}]$, which is related to the strain-rate tensor $[e_{ij}]$ by the specific constitutive equation the liquid obeys.

The dilute polymer solutions of interest may be slightly viscoelastic (ref. 18). To predict their behavior involving viscoelastic effects, two generally accepted models for viscoelastic fluids are analyzed in the following.

Second-Order Fluid Model

A second-order fluid model proposed by Markovitz and Coleman (ref. 19) has the constitutive equation of the form

$$\sigma_{ij} = \mu e_{ij}^{(1)} + \alpha e_{ij}^{(2)} + \beta e_{ik}^{(1)} e_{kj}^{(1)} \tag{7}$$

where μ is the Newtonian viscosity, α and β are material constants, and

$$e_{ij}^{(1)} = v_{i,j} + v_{j,i}$$

$$e_{ij}^{(n)} = \frac{De_{ij}^{(n-1)}}{Dt} + e_{ik}^{(n-1)} v_{k,j} + e_{jk}^{(n-1)} v_{k,i}$$

For the present problem, the strain-rate tensor is

$$[e_{ij}] = \begin{bmatrix} \dfrac{\partial u}{\partial r} & 0 & 0 \\ 0 & \dfrac{u}{r} & 0 \\ 0 & 0 & \dfrac{u}{r} \end{bmatrix} \tag{8}$$

By substituting equation (8) into equation (7), it can be noted that the second normal stress difference vanishes:

$$\sigma_{\theta\theta}-\sigma_{\varphi\varphi}=0$$

and hence the relation

$$2\alpha+\beta=0 \tag{9}$$

is used to simplify the analysis (ref. 19). By using equations (4), (7), and (9), equation (6) becomes

$$\rho\frac{\partial u}{\partial t}+\rho u\frac{\partial u}{\partial r}=-\frac{\partial p}{\partial r}-\frac{8\alpha}{3}\frac{\partial u}{\partial r}\cdot\frac{\partial^2 u}{\partial r^2} \tag{10}$$

Substituting equation (5) into equation (10) and integrating over (R, ∞), the result is

$$R\ddot{R}+\frac{3}{2}\dot{R}^2-\frac{16\gamma}{3}\left(\frac{\dot{R}}{R}\right)^2=\frac{P(R)-P(\infty)}{\rho} \tag{11}$$

where $(\dot{}) = d/dt$, $\gamma=\alpha/\rho$ with a dimension of [length]^2 and $P(\infty)=P_a$ is the constant pressure at infinity. The hydrostatic pressure $P(R)$ is eliminated by applying the boundary condition at the bubble wall; i.e., at $r=R$,

$$\begin{aligned}P_v-\frac{2\sigma}{R}&=-\sigma_{rr}(R)\\&=P(R)-2\mu\left[\frac{\partial u}{\partial r}\right]_{r=R}-2\alpha\left[\frac{\partial^2 u}{\partial t\partial r}+u\frac{\partial^2 u}{\partial r^2}-2\left(\frac{\partial u}{\partial r}\right)^2\right]_{r=R}\end{aligned} \tag{12}$$

where P_v is the vapor pressure inside the bubble and σ is the surface tension.

Combining equations (11) and (12), the equation governing the collapsing process of the bubble is obtained.

$$\left(R+\frac{4\gamma}{R}\right)\ddot{R}+\left(\frac{3}{2}+\frac{20\gamma}{3R^2}\right)\dot{R}^2+4\nu\frac{\dot{R}}{R}=\frac{P_v-P_a-(2\sigma/R)}{\rho} \tag{13}$$

where $\nu=\mu/\rho$ is the kinematic viscosity of the fluid. For the special case of $\gamma=0$, equation (13) reduces to the classical bubble equation in a Newtonian fluid (ref. 11).

$$R\ddot{R}+\frac{3}{2}\dot{R}^2+4\nu\frac{\dot{R}}{R}=\frac{P_v-P_a-(2\sigma/R)}{\rho} \tag{13'}$$

From the prediction of molecular theory, γ or α is negative (ref. 20). Consequently, equation (13) shows that under the same pressure difference P_v-P_a, the bubble in a non-Newtonian fluid obeying the constitutive

relation, equation (7), of the second-order fluid model will collapse more rapidly than in the Newtonian fluid.

Oldroyd Three-Constant Fluid Model

Oldroyd (ref. 21) suggested the following constitutive equation for a viscoelastic fluid:

$$\sigma_{ij}+\lambda_1\left[\frac{\partial\sigma_{ij}}{\partial t}+v_k\frac{\partial\sigma_{ij}}{\partial x_k}-\sigma_{ik}e_{jk}-\sigma_{kj}e_{ik}\right]=2\mu\left[e_{ij}+\lambda_2\left(\frac{\partial e_{ij}}{\partial t}+v_k\frac{\partial e_{ij}}{\partial x_k}-2e_{ik}e_{kj}\right)\right] \tag{14}$$

where λ_1 and λ_2 are two material constants, both having the dimension of [time] and a positive sign.

Due to the special form of the strain-rate tensor in this problem, the shear stress components $\sigma_{r\theta}$, $\sigma_{\theta\varphi}$, and $\sigma_{r\varphi}$ vanish, and the normal stress components $\sigma_{\theta\theta}$ and $\sigma_{\varphi\varphi}$ are equal. Using equation (5), the stress components σ_{rr} and $\sigma_{\phi\phi}$ are determined by the following relations:

$$\frac{\partial\sigma_{rr}}{\partial t}+\frac{R^2\dot{R}}{r^2}\frac{\partial\sigma_{rr}}{\partial r}+\left(\frac{1}{\lambda_1}+4\frac{R^2\dot{R}}{r^3}\right)\sigma_{rr}=-\frac{4\mu}{\lambda_1}\cdot\frac{R^2\dot{R}}{r^3}\left[1+\lambda_2\left(\frac{\ddot{R}}{\dot{R}}+\frac{2\dot{R}}{R}+\frac{R^2\dot{R}}{r^3}\right)\right] \tag{15}$$

$$\frac{\partial\sigma_{\varphi\varphi}}{\partial t}+\frac{R^2\dot{R}}{r^2}\frac{\partial\sigma_{\varphi\varphi}}{\partial r}+\left(\frac{1}{\lambda_1}-2\frac{R^2\dot{R}}{r^3}\right)\sigma_{\varphi\varphi}=\frac{2\mu}{\lambda_1}\cdot\frac{R^2\dot{R}}{r^3}\left[1+\lambda_2\left(\frac{\ddot{R}}{\dot{R}}+\frac{2\dot{R}}{R}-5\frac{R^2\dot{R}}{r^3}\right)\right] \tag{16}$$

Equations (6), (15), and (16) are thus the governing equations for the bubble-collapsing problem. It was found convenient to introduce the transformation to Lagrangian coordinates (ref. 10):

$$h=\tfrac{1}{3}[r^3-R^3(t)] \tag{17}$$

Then equations (15) and (16) become

$$\frac{d\sigma_{rr}}{dt}+\left(\frac{1}{\lambda_1}+4\frac{R^2\dot{R}}{r^3}\right)\sigma_{rr}=-\frac{4\mu}{\lambda_1}\cdot\frac{R^2\dot{R}}{r^3}\left[1+\lambda_2\left(\frac{\ddot{R}}{\dot{R}}+\frac{2\dot{R}}{R}+\frac{R^2\dot{R}}{r^3}\right)\right] \tag{18}$$

$$\frac{d\sigma_{\varphi\varphi}}{dt}+\left(\frac{1}{\lambda_1}-2\frac{R^2\dot{R}}{r^3}\right)\sigma_{\varphi\varphi}=\frac{2\mu}{\lambda_1}\cdot\frac{R^2\dot{R}}{r^3}\left[1+\lambda_2\left(\frac{\ddot{R}}{\dot{R}}+\frac{2\dot{R}}{R}-5\frac{R^2\dot{R}}{r^3}\right)\right] \tag{19}$$

which are readily integrated to obtain

$$\sigma_{rr}(h,t)=-\frac{4\mu}{\lambda_1}\int_0^t e^{(\tau-t)/\lambda_1}R^2(\tau)\dot{R}(\tau)\left\{\frac{[3h+R^3(\tau)]^{1/3}}{[3h+R^3(t)]^{4/3}}\right\}\{1+\lambda_2 M_{rr}(h,\tau)\}\,d\tau \tag{20}$$

$$\sigma_{\varphi\varphi}(h,t)=\frac{2\mu}{\lambda_1}\int_0^t e^{(\tau-t)/\lambda_1}R^2(\tau)\dot{R}(\tau)\left\{\frac{[3h+R^3(t)]^{2/3}}{[3h+R^3(\tau)]^{5/3}}\right\}\{1+\lambda_2 M_{\varphi\varphi}(h,\tau)\}\,d\tau \tag{21}$$

where

$$M_{rr}(h,\tau)=\frac{\ddot{R}(\tau)}{\dot{R}(\tau)}+\frac{2\dot{R}(\tau)}{R(\tau)}+\frac{R^2(\tau)\dot{R}(\tau)}{3h+R^3(\tau)} \tag{22}$$

$$M_{\varphi\varphi}(h,\tau)=\frac{\ddot{R}(\tau)}{\dot{R}(\tau)}+\frac{2\dot{R}(\tau)}{R(\tau)}-5\frac{R^2(\tau)\dot{R}(\tau)}{3h+R^3(\tau)} \tag{23}$$

Substituting equations (20) and (21) into equation (6) written in terms of the new coordinates (h,t), and integrating over the range from $h=0(r=R)$ to $h=\infty\,(r=\infty)$, the result is

$$\rho(R\ddot{R}+\tfrac{3}{2}\dot{R}^2)+4\mu\frac{\dot{R}}{R}=P_v-P_a-\frac{2\sigma}{R}+\frac{2\mu}{\lambda_1}(\lambda_1-\lambda_2)$$
$$\times\int_0^t e^{(\tau-t)/\lambda_1}\left[\left(1+\frac{R^3(\tau)}{R^3(t)}\right)\frac{\ddot{R}(\tau)}{R(t)}+3\frac{R^2(\tau)}{R^4(t)}\dot{R}(\tau)^2\right]d\tau \tag{24}$$

The first term in the integral of equation (24) is integrated by parts, and by using the initial condition

$$\dot{R}(0)=0 \tag{25}$$

for the bubble-collapse problem, equation (24) reduces to the form

$$R\ddot{R}+\frac{3}{2}\dot{R}^2+4\nu\frac{\lambda_2}{\lambda_1}\frac{\dot{R}}{R}+\frac{P_a-P_v+(2\sigma/R)}{\rho}$$
$$=-\frac{2\nu}{\lambda_1}\left(1-\frac{\lambda_2}{\lambda_1}\right)\int_0^t e^{(\tau-t)/\lambda_1}\frac{\dot{R}(\tau)}{R(t)}\left[1+\frac{R^3(\tau)}{R^3(t)}\right]d\tau \tag{26}$$

For the Newtonian case, $\lambda_2/\lambda_1\to 1$ and equation (26) again reduces to equation (13′). In general, λ_2 is less than λ_1. With the appropriate interpretation of the material constants μ, λ_1, and λ_2 (ref. 22), it is shown that the third term on the left of equation (26), the viscous damping term, is not changed with respect to the Newtonian case. The viscoelastic memory integral on the right-hand side then appears to have the effect of slowing down the collapse. However, by a dimensional analysis it can be shown that, in the situation of a collapsing bubble, the magnitude of the viscoelastic correction term—as well as that of the viscous damping term—is too small to affect the collapse process in any significant way.

While the two constitutive relations used give different results, the authors believe that the conclusion deduced from the Oldroyd fluid will be more applicable in a real physical situation in the viscoelastic fluids. It has been suggested that the Oldroyd model is superior to the second-order model at higher strain rates (ref. 23). Indeed, the inadequacy of the second-order fluid model is not surprising, since it is generally known to be a poor model for unsteady flows involving short deformation periods (ref. 24), in which cases the results could lead to paradoxes (ref. 25) and questionable mathematical solutions.

EXPERIMENTAL PROCEDURE

A cubical lucite tank 30 centimeters on a side was used to contain the liquid. The flat walls avoided optical problems, and the tank was large enough that the 1-centimeter-diameter, spark-generated bubbles would not suffer from wall proximity effects. Small tungsten wires were used for the underwater spark gap. These may be seen in the bubble photographs of figure 2. It may be noted that there is negligible departure from a spherical shape. The spark was formed by discharge of a 0.04-μF capacitor charged to 14 000 volts through a 5C22 hydrogen thyratron which allowed current to flow in one direction only, so that there was a single pulse of about a microsecond duration without any subsequent current oscillations. This was important in order to obtain essentially a delta function of heat energy to grow the bubble in a steady one-atmosphere pressure field. These conditions are essential to simplify the analysis. The bubble photographs of figure 2 were taken at a repetition rate of 10 000 per second or 100 microseconds between frames. The bubbles were back-lighted by a xenon flash lamp operating at $\frac{1}{4}$ joule per flash and a 1-microsecond duration. The pulsing was also done by a 5C22 hydrogen thyratron. It was realized that such a slow rate would not give much detail for the radius/time curve, but the high-speed photographic equipment had not yet been reassembled. It was thought that any gross effects caused by the polymer solutions would still be evident.

The spark gap which generated the bubble was fired at random times with respect to the photographic frames, and at least five runs were made for each solution. This is evident from the bright spot caused by the spark at the beginning of each sequence. (Apparent bright spots near the bubbles' centers are due only to the back-lighting.) The pictures were taken on a rotating-drum streak camera without any mechanical shutter or optical compensation for the speed of the moving 35–mm film. As can be seen from these contact prints and the accompanying scale, the film speed was about 12 000 centimeters per second. Tri–X film and D–19 developer were used, and the lens was of 10-inch focal length stopped

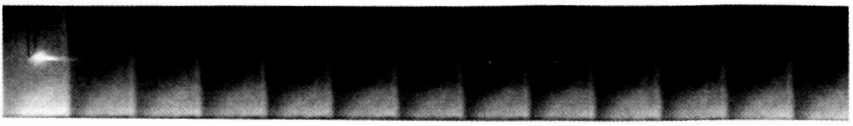

a.—*Water.*

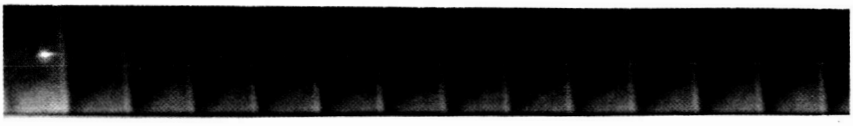

b.—*Fresh 100-ppm Polyox.*

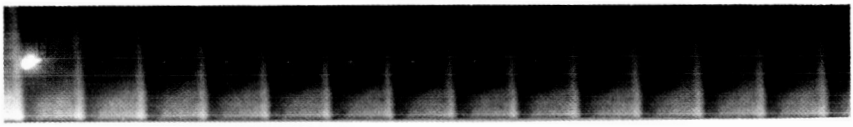

c.—*Aged 100-ppm Polyox.*

d.—*Aged 1000-ppm Polyox.*

e.—*Fresh 300-ppm Guar Gum.*

f.—*Scale in centimeters.*

FIGURE 2.—*Growth and collapse of spark-generated bubbles in various solutions (picture rate is 10 000 per second).*

down to $f16$. All runs were made at one-atmosphere pressure; hence no jet formation was observed, in contrast to earlier work performed by Benjamin and Ellis (ref. 16) at the University of Cambridge. The difference was, of course, due to the lower ambient pressures used in the latter experiments. The ratio of pressure gradient to pressure is the pertinent parameter for jet formation in bubble collapse far from boundaries. Bubble photographs for five runs of each solution (fig. 2 shows representative sequences) were measured on a precision traveling microscope with a readout of 10^{-4} centimeter per division.

RESULTS AND DISCUSSION

The experimental results for the radius/time curves of the different solutions are plotted as points on figures 3, 4, 5, 6, and 7. The dimensionless radius, R/R_0 (where R_0 is the maximum radius), is the ordinate; the dimensionless collapse time, t/τ (where τ is the Rayleigh theoretical collapse time for a bubble of the particular R_0 observed), is the abscissa. The solid lines are theoretical curves obtained on a computer for the second-order fluid model with $\gamma = 0$ (which reduces to the Rayleigh theory) and $\gamma = -0.01$. Time was not available to compute a corresponding curve for the Oldroyd model.

It may be seen that figure 3, the case for water, followed the correct Rayleigh curve quite well, which was taken to be a good check on the

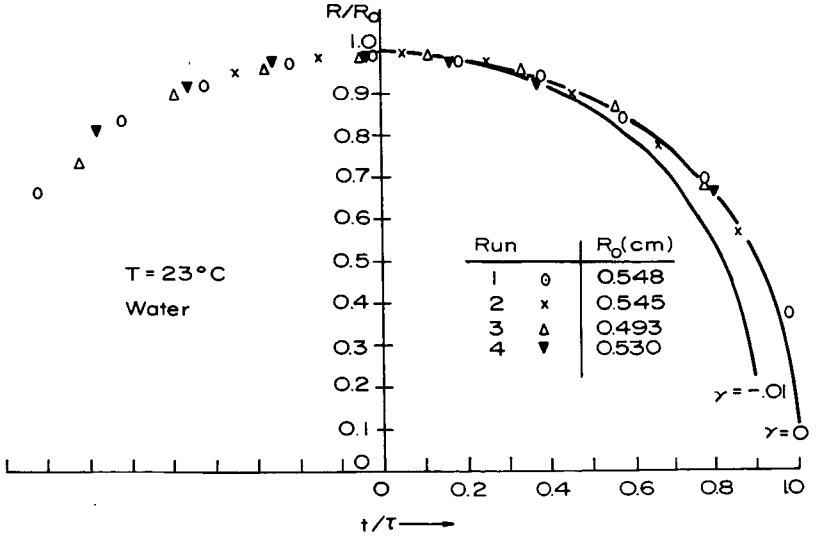

FIGURE 3.—*Experimental points and theoretical dimensionless bubble collapse curves for water under atmospheric pressure.*

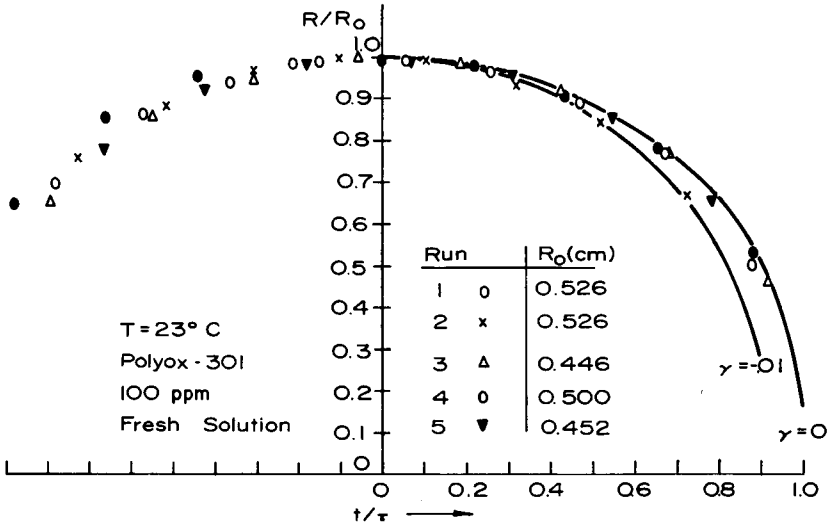

FIGURE 4.—*Experimental points and theoretical dimensionless bubble collapse curves for fresh 100–ppm Polyox under atmospheric pressure.*

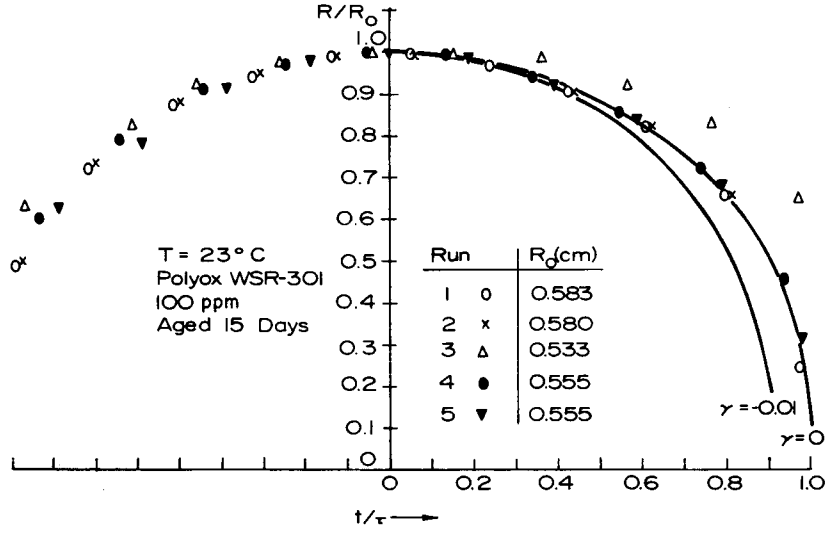

FIGURE 5.—*Experimental points and theoretical dimensionless bubble collapse curves for aged 100–ppm Polyox under atmospheric pressure.*

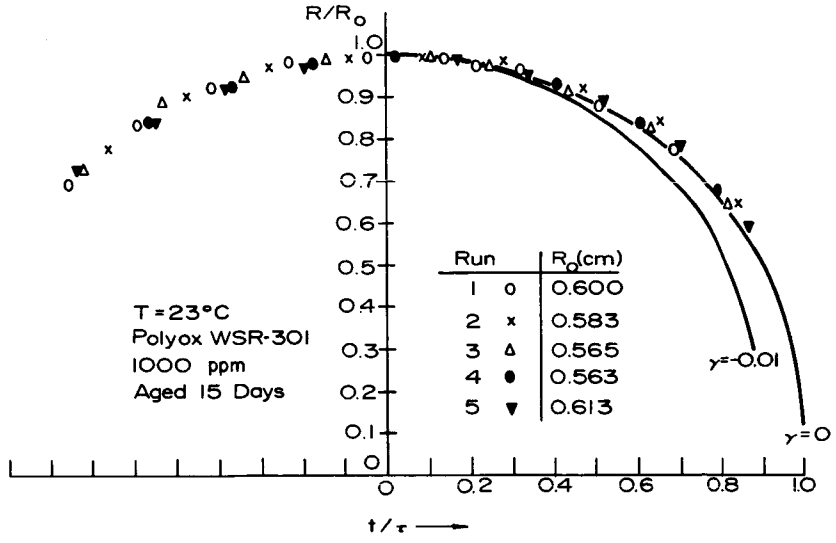

FIGURE 6.—*Experimental points and theoretical dimensionless bubble collapse curves for aged 1000–ppm Polyox under atmospheric pressure.*

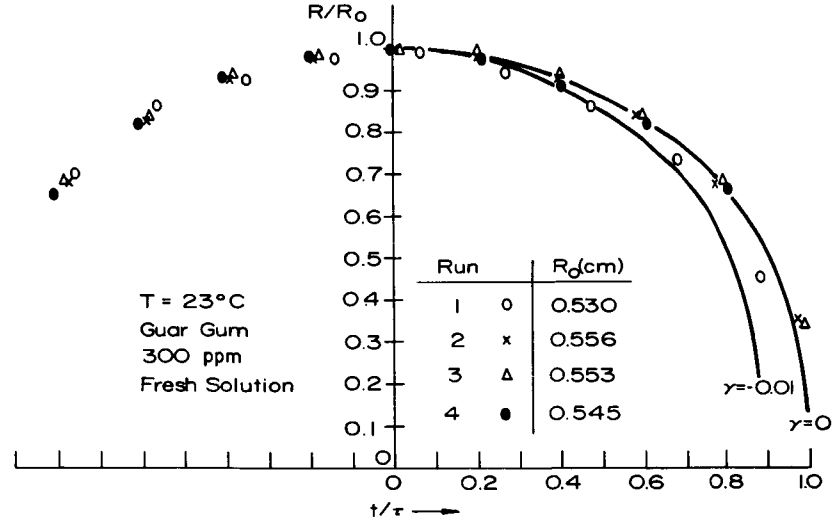

FIGURE 7.—*Experimental points and theoretical dimensionless bubble collapse curves for fresh 300–ppm Guar Gum under atmospheric pressure.*

validity of the experimental method. However, the polymer solutions also seemed to follow this curve fairly well. The exceptions were run 2 of the fresh 100–ppm Polyox series (fig. 4), which collapsed faster in agreement with second-order theory, and run 3 of the aged 100–ppm Polyox (fig. 5), which collapsed more slowly than water. It is regretted that only five runs for each system were made, but time was not available. However, with four runs out of five agreeing, it is felt that these single runs should be discounted.

SUMMARY AND CONCLUSIONS

Theoretical expressions for a spherical cavity collapsing in a stationary infinite fluid are derived for liquid constitutive equations of both the second-order and Oldroyd types. These reduce to the classical Rayleigh result if the non-Newtonian parameters are set to zero. Both models predict that bubble collapse will be different relative to the case for water; however, the difference will be very small due to the low concentrations used.

Experimentally obtained collapse curves show little difference from water and thus indicate that—for the concentrations used and for the resolution of the experiment—the effect of dilute polymers on local bubble dynamics is negligible. It is reasonable to expect normal stress differences to have some effect on bubble dynamics, but preliminary computer results show their maximum magnitude to be only about 1 percent of ambient pressure for these experiments. This tends to support the authors' present view that cavitation suppression by polymers is due to changes of pressure in flow fields. Future work is planned to properly measure the tractions on solid surfaces in flow, since this appears to be of prime importance.

REFERENCES

1. Ellis, A. T., and J. W. Hoyt, *Some Effects of Macromolecules on Cavitation Inception.* ASME 1968 Cavitation Forum, ASME Fluids Engineering Conference (Philadelphia), May 1968, pp. 2–3.
2. Ellis, A. T., J. G. Waugh, and R. Y. Ting, Cavitation Suppression and Stress Effects in High-Speed Flows of Water with Dilute Macromolecule Additives. *Trans. ASME, J. Basic Eng.*, Series D, September 1970, p. 459.
3. Ellis, A. T., B. S. Barnard, and M. E. Slater, *The Unsteady Flow Cavitation Tunnel at the California Institute of Technology.* ASME Symposium on Cavitation Research Facilities and Techniques, May 1964.
4. Stewart, H. J., unpublished work from Guggenheim Aeronautical Laboratory, Cal Tech, circa 1950.
5. Tsien, H. S., On the Design of the Contraction Cone for a Wind Tunnel. *J. Aeron. Sci.*, Vol. 10, 1943, p. 68.

6. TANNER, R. I., AND A. C. PIPKIN, Intrinsic Errors in Pressure-Hole Measurements. *Trans. Soc. Rheology*, Vol. 13, No. 4, 1969, p. 471.
7. LUMLEY, J. L., Drag Reduction by Additives. *Annual Reviews of Fluid Mechanics*, W. Sears and M. Van Dyke, eds., Vol. 1, 1969, p. 367.
8. TANNER, R. I., personal communication.
9. RAYLEIGH, The Pressure Developed in a Liquid During the Collapse of a Spherical Cavity. *Phil. Mag.*, 34:94, 1917.
10. EPSTEIN, P. R., AND M. S. PLESSET, Stability of Gas Bubbles in Liquid-Gas Solutions. *J. Chem. Phys.*, Vol. 18, 1950, p. 1505.
11. PLESSET, M. S., AND S. A. ZWICK, On the Dynamics of Small Vapor Bubbles in Liquids. *J. Math. Phys.*, Vol. 33, No. 4, 1955.
12. DERGARABEDIAN, P., Observations on Bubble Growths in Various Superheated Liquids. *J. Fluid Mech.*, Vol. 9, Part 1, 1960, pp. 39–48.
13. PLESSET, M. S., AND T. P. MITCHELL, On the Stability of the Spherical Shape of a Vapor Cavity in a Liquid. *Quart. Appl. Math.*, Vol. 13, 1956, p. 419.
14. MITCHELL, T. P., AND F. T. HAMMITT, *Collapse of a Spherical Bubble in a Pressure Gradient.* ASME Cavitation Symposium, 1970.
15. ELLIS, A. T., AND C. F. NAUDE, On the Mechanism of Cavitation Damage by Nonhemispherical Cavities Collapsing in Contact With a Solid Boundary. *Trans. ASME, J. Basic Eng.*, Vol. 83, 1961, p. 648.
16. BENJAMIN, T. B., AND A. T. ELLIS, The Collapse of Cavitation Bubbles and the Pressures Thereby Produced Against Solid Boundaries. *Phil. Trans. Roy. Soc. London*, Series A, No. 1110, Vol. 260, July 1966, pp. 221–240.
17. PLESSET, M. S., The Dynamics of Cavitation Bubbles. *J. Appl. Mech.*, September 1949, p. 277.
18. METZNER, A. B., AND M. G. PARK, Turbulent Flow Characteristics of Viscoelastic Fluids. *J. Fluid Mech.*, Vol. 20, 1964, p. 291.
19. MARKOVITZ, H., AND B. D. COLEMAN, Incompressible Second-Order Fluid. *Advances Appl. Mech.*, 1964, p. 69.
20. SINGH, K., *Non-Newtonian Effects on the Turbulent Energy Spectrum Function.* Ph.D. thesis, Penn. State U., 1966.
21. OLDROYD, J. G., On the Formulation of Rheological Equations of State. *Proc. Roy. Soc. (London)*, Series A, Vol. 200, 1950, p. 523.
22. LUMLEY, J. L., personal communication.
23. STREET, J. R., The Rheology of Phase Growth in Elastic Liquids. *Trans. Soc. Rheology*, 12:1, 1968, p. 103.
24. METZNER, A. B., J. L. WHITE, AND M. M. DENN, Significance of the Deborah Number. *Am. Inst. Chem. Engrs. J.*, 12:5, 1966, p. 863.
25. COLEMAN, B. D., R. J. DUFFIN, AND V. J. MIZEL, Instability, Uniqueness, and Nonexistence Theorems for the Equation $u_t = u_{xx} - u_{xtx}$ on a Strip. *Arch. Rat. Mech. Anal.*, Vol. 19, 1965, pp. 100.

DISCUSSION

J. L. LUMLEY (The Pennsylvania State University): The authors, Ellis and Ting, are to be commended for a particularly clear combination of calculation and experimental work. I agree fully with the conclusions which they draw therefrom. At the same time, I feel that the analytical basis on which their conclusions rest is somewhat open to question and would not provide a suitable basis for future work.

My comments relate primarily to the choice of constitutive relation. The second-order fluid model used by the authors is likely to be a poor model, since it includes only in a rudimentary way the effect of molecular extension, which seems likely (ref. D–1) to be responsible for the large effects observed in these very dilute solutions. A much better model is provided by the Oldroyd equation (ref. D–2), which can be shown to be based on a dumbbell model of the molecule (the form of the equation quoted by the authors is correct only in an irrotational flow; see ref. D–2 for the complete equations). In this way, the constants used by the author may be identified as

$$\left.\begin{aligned} \lambda_1 &= T \\ \lambda_2 &= T/(1+c[\eta]) \\ \mu &= \mu_0(1+c[\eta]) \end{aligned}\right\} \qquad \text{(D–1)}$$

where T is the molecular terminal relaxation time, c is the concentration, $[\eta]$ is the intrinsic viscosity, and μ_0 is the solvent viscosity. Substitution of these values into the authors' final form (eq. (26)) indicates that the coefficient of the viscous damping term

$$4\frac{\mu}{\rho}\frac{\lambda_2}{\lambda_1} = 4\frac{\mu_0}{\rho} \qquad \text{(D–2)}$$

is the value for the solvent alone, so that the viscous damping is unchanged. Hence, the only effect lies in the viscoelastic memory integral, having a coefficient of

$$\frac{2\mu_0 c[\eta]}{\rho T} \qquad \text{(D–3)}$$

The authors' conclusion that this would slow the collapse, but is ordinarily

quite small, certainly appears to apply during the early stages of the collapse; as the bubble closes, however, and the strain rate rises to quite large values (relative to $1/2T$), this term may slow the final stages appreciably. Numerical calculations appear to be warranted.

The same remarks relative to the constitutive equation can be made in connection with the authors' calculation of the pressure in a contraction. In the quasi-steady case, using the Oldroyd equation, it is possible (refs. D–3 and D–4) to obtain an analog of the Bernoulli equation applicable on the centerline:

$$P = P_N + \frac{\mu_0 c[\eta]}{T}\left\{\frac{2ST}{(1-2ST)(1+ST)} + \frac{2}{3}\ln\left(\frac{1-2ST}{1+ST}\right)\right\} \quad \text{(D–4)}$$

where S is the local strain rate ($2ST<1$) and the additional term can be shown always to be positive, in agreement with the authors' observations. From the derivation of equation (D–4), it appears to be a bound (for an Oldroyd fluid) in the sense that the deviation from P_N cannot be more positive than this.

R. E. A. ARNDT (The Pennsylvania State University): The authors are to be congratulated on presenting an excellent sequel to their original work (ref. 2), which demonstrated a non-Newtonian effect on cavitation in essentially irrotational flow. In the discussion of that previous paper, it was pointed out that the observed delay of cavitation inception could be a result of either a reorientation of the flow field or a change in the bubble dynamics. Apparently this paper is the first in a series of steps toward isolating the one or more mechanisms involved.

With this in mind, one must focus attention on the basic question at hand—namely, what causes the observed reduction in the value of incipient cavitation index based on upstream velocity and pressure? This paper considers the possibility of an effect on the bubble dynamics by polymer addition. Presumably such an effect is small, and this discussant's intuition agrees with the authors' conclusion on the point. This conclusion, however, is based on the evidence that relatively large spark-generated bubbles collapse under atmospheric pressure in a manner which appears to be relatively insensitive to the presence of small quantities of polymer. Two questions immediately arise in extending this result to consideration of cavitation inception: First, is there a "size effect" for the onset of viscoelastic phenomena in bubble dynamics? Second, is there an effect on nuclei distribution with the addition of polymers? What this discussant has in mind is that a spherical bubble expansion or collapse induces an axisymmetric strain, the magnitude of which probably increases with a decrease in bubble size. Presumably a critical value of rate of strain must be reached before viscoelastic phenomena become evident, and experiments with large bubbles may not be in the right size range for

observation of any effect. This second question is not the subject of this paper and will require further investigation. As with any good piece of research, the paper has generated several new questions to be answered.

M. S. PLESSET (California Institute of Technology): Ellis and Ting have given convincing evidence that dilute polymer solutions in water do not have a significant effect on the collapse of cavitation bubbles. It is indeed of interest that their measurements show radius/time curves that are essentially the same as those which they observed in pure water.

Also of importance is the authors' theoretical analysis, which points in the direction of faster collapse than for pure water. Here they do not find experimental evidence that indicates any speeding up of the collapse in the polymer solutions.

It is perhaps not surprising that the dilute polymer solutions show no significant effect in cavity collapse. We are familiar with the fact that ordinary viscous effects are not important for growth or collapse behavior in liquids of low viscosity such as water. It is, however, useful to have this result as well for the non-Newtonian liquids used by the authors.

Some experiments performed in our laboratory at the California Institute of Technology support the conclusion of the present paper. Using some polymer solutions prepared by Dr. Hoyt of the Naval Undersea Research and Development Laboratory, we measured cavitation damage rates in an oscillating magnetostrictive device. We observed no difference between the damage rate with pure water and the damage rate with the dilute polymer solution. In the light of the study of Ellis and Ting this observation is very satisfying. However, our experimental findings with the oscillating magnetostrictive device are not of themselves conclusive, since it is to be expected that the pressure oscillations generated in those experiments would produce some degradation of the drag-reducing additive.

ELLIS AND TING (authors): We agree with Dr. Arndt and Dr. Lumley that the scales in our experiment are not such as to show up non-Newtonian effects until later stages in the collapse, and this is also evident from our theory. However, the assumption of spherical symmetry would be invalid if we observed the collapse at later stages in these experiments.

We also agree that the Oldroyd constitutive equation is more applicable than the second-order fluid model. That is why we derived the bubble collapse equation using the Oldroyd model. The second-order model was also included for comparison in the bubble problem and was used for obtaining the venturi pressure drop. It is agreed that the expression given by Dr. Lumley is probably more accurate, but the qualitative results of both models are the same—including the algebraic sign of the pressure correction term.

It should be pointed out that the rotational terms in the Oldroyd equation are well known, but were not included here because the flow considered is irrotational.

Dr. Lumley, in his discussion, gave an interpretation of μ, λ_1, and λ_2 based on a molecular model which was unknown to the authors at the time the paper was written. This interpretation leads to the conclusion that bubble collapse will be slowed down relative to collapse in water. However, the difference could still be too small for our experiment to detect, and there is no contradiction to the results obtained by Dr. Plesset even if degradation was not present.

REFERENCES

D–1. LUMLEY, J. L., Drag Reduction by Additives. *Annual Review of Fluid Mechanics*, Vol. 1, 1969, p. 367.

D–2. LUMLEY, J. L., *Applicability of the Oldroyd Constitutive Equation to Flow of Dilute Polymer Solutions*. Internal Memorandum, Ordnance Res. Lab, Penn. State U. (to be issued).

D–3. LUMLEY, J. L., *A Centerline Bernoulli Equation for Quasi-Steady Dilute Polymer Flow*. Internal Memorandum, Ordnance Res. Lab, Penn. State U. (to be issued).

D–4. LUMLEY, J. L., *On the Solution of Equations Describing Small Scale Deformation*. Technical Memorandum 503–09, Ordnance Res. Lab, Penn. State U., August 12, 1970.